Research paper

HAX1 is a novel binding partner of Che-1/AATF. Implications in oxidative stress cell response

Cinzia Pisani [a,*], Annalisa Onori [a], Francesca Gabanella [b], Simona Iezzi [c], Roberta De Angelis [d], Maurizio Fanciulli [c], Andrea Colizza [e], Marco de Vincentiis [e], Maria Grazia Di Certo [b], Claudio Passananti [a,*], Nicoletta Corbi [a,*]

[a] CNR-Institute of Molecular Biology and Pathology, Department of Molecular Medicine, Sapienza University of Rome, Viale Regina Elena 291, 00161 Rome, Italy
[b] CNR-Institute of Biochemistry and Cell Biology, Department of Sense Organs, Sapienza University of Rome, Viale del Policlinico 155, 00161 Rome, Italy
[c] SAFU Unit, Department of Research and Advanced Technologies, Translational Research Area, IRCCS Regina Elena National Cancer Institute, Via Elio Chianesi 53, 00144 Rome, Italy
[d] ISPRA, Italian National Institute for Environmental Protection and Research, Via Vitaliano Brancati 48, 00144 Rome, Italy
[e] Department of Sense Organs, Sapienza University of Rome, Viale del Policlinico 155, 00161 Rome, Italy

ABSTRACT

HAX1 is a multifunctional protein involved in the antagonism of apoptosis in cellular response to oxidative stress. In the present study we identified HAX1 as a novel binding partner for Che-1/AATF, a pro-survival factor which plays a crucial role in fundamental processes, including response to multiple stresses and apoptosis. HAX1 and Che-1 proteins show extensive colocalization in mitochondria and we demonstrated that their association is strengthened after oxidative stress stimuli. Interestingly, in MCF-7 cells, resembling luminal estrogen receptor (ER) positive breast cancer, we found that Che-1 depletion correlates with decreased HAX1 mRNA and protein levels, and this event is not significantly affected by oxidative stress induction. Furthermore, we observed an enhancement of the previously reported interaction between HAX1 and estrogen receptor alpha (ERα) upon H_2O_2 treatment. These results indicate the two anti-apoptotic proteins HAX1 and Che-1 as coordinated players in cellular response to oxidative stress with a potential role in estrogen sensitive breast cancer cells.

1. Introduction

HAX1 (HCLS1-associated protein X-1) is an anti-apoptotic protein ubiquitously expressed in various tissues and tumors [1,2]. HAX1 is involved in many cellular processes and functions, including regulation of apoptosis, cell proliferation [3–5], cell adhesion and migration [6–9], endocytosis [8], autophagy [10], ribosome biogenesis [11] and mRNA metabolism [11–14]. Mutations in the human HAX1 gene are responsible for autosomal recessive severe congenital neutropenia (SCN or Kostmann disease) and neurological abnormalities, mainly resulting from defective mitochondrial control of apoptosis [15,16]. HAX1 was found to mainly localize in mitochondria and has been reported to be critical in maintaining the inner mitochondrial membrane potential [15]. It is also localized in endoplasmic reticulum, nucleus, plasma membrane/on the leading edge of lamellipodia and cytoplasmic vesicles/granules, as P-bodies [17]. HAX1 participates in the regulation of apoptosis through attenuation of the damaged signals from mitochondria and endoplasmic reticulum [18–26]. In the antioxidative stress response HAX1 exerts its anti-apoptotic role through different pathways not fully clarified. It can affect the Akt1/MDM2/p53 axis and the expression of p21, Bax and p53 proteins to participate in cell apoptosis control [27]. Moreover, it has been recently reported that HAX1 in response to oxidative or genotoxic stress activates the non-receptor tyrosine kinase c-Abl, thereby promoting c-Abl-mediated activation of catalase and glutathione peroxidase resulting in reactive oxygen species (ROS) clearance [28]. Deregulation of the expression levels and subcellular distribution of HAX1 is associated with the development and progression of severe diseases, including cancer and psoriasis [29]. HAX1 overexpression was reported in several cancers [5,8,30–32], including breast cancer and its expression analysis in correlation to metastasis revealed its significant prognostic value for luminal estrogen receptor positive (ER+) breast cancer metastasis [2,4,8,33]. It has been reported that HAX1 forms a complex with prohibitin 2 (PHB2) that in the presence of Estrogen receptor alpha (ERα) and estradiol, translocates

to the nucleus, suggesting a link between HAX1 and estrogen-receptor signaling [17,34]. Moreover, a possible involvement of HAX1 in estrogen signaling is also supported by microarray studies, which classified HAX1 as estrogen-responsive [35,36]. Of note, HAX1 was shown to directly bind ERα that represents a pro-metastatic factor [4,37].

Pathologic overexpression of HAX1 was observed also in psoriasis, a severe inflammatory disease characterized by increased proliferation and dysfunctional apoptosis of keratinocytes [38,39]. Interestingly, we recently reported that HAX1 interacts with the psoriasis candidate Coiled-Coil alpha-Helical Rod 1 (CCHCR1) protein and importantly we found that both proteins are associated to specific mRNAs [12].

In the present study, HAX1 was determined to be a novel binding partner of Apoptosis Antagonizing Transcription Factor (AATF)/Che-1 protein. Che-1 is an RNA polymerase (RNA Pol) I and II interacting protein highly conserved during evolution [40,41]. It is involved in many fundamental cellular processes, such as transcriptional regulation, ribosome biogenesis, cell-cycle and apoptosis control, cellular response to DNA damage and stress, RNA binding and inflammatory response activation [42–46]. At the cellular level, Che-1 predominantly shows a nuclear and nucleolar localization [41]. However, Che-1 protein distribution has been also reported in centrosomes, focal adhesion, Golgi apparatus, and mitochondria [47–50]. Che-1 protects cells from multiple stress stimuli such as DNA damage, endoplasmic reticulum (ER) stress, hypoxia, or glucose deprivation by inducing cell cycle arrest, autophagy, or apoptosis inhibition. The critical role of Che-1 in the modulation of apoptosis can be played either by activation of anti-apoptotic pathways or by inhibition of pro-apoptotic pathways [42]. The interaction of Che-1 with different proteins such as DAP-like kinase (Dlk), prostate apoptosis response 4 (Par-4), and neurotrophin receptor-interacting MAGE homolog (NRAGE/MAGED1) resulted in the inhibition of apoptosis [43,51–53]. In addition, Che-1 shows a protective role in human kidney proximal tubule cells, where this protein has been observed to counteract apoptotic cell death following induced-renal injury by preserving mitochondrial function and reducing oxidative damage [54]. Over the last years, several pieces of evidence indicate that Che-1 serves as a critical regulator in various cancers and promotes tumorigenesis by protecting cancer cells from apoptosis induction, favoring cell proliferation, or promoting cell survival by autophagy [44,55–58]. In breast cancer Che-1 is upregulated and its gene silencing leads to stimulation of apoptotic cell death via upregulation of proapoptotic genes and downregulation of ERα, a key factor in breast cancer development [42,59]. Of importance, Bruno and colleagues have recently shown that Che-1 depletion leads to downregulation of HAX1 in Multiple Myeloma [44].

In this study, we show that HAX1 interacts with Che-1 and that Che-1 depletion correlates with downregulation of HAX1 in MCF-7 cells. HAX1 and Che-1 proteins colocalize mainly in mitochondria and notably we found that their association is strengthened after oxidative stress stimuli in MCF-7 cells. Interestingly, we observed an enhancement also of the previously reported interaction between HAX1 and ERα, upon H_2O_2 treatment [37]. These results suggest that the two anti-apoptotic proteins HAX1 and Che-1 cooperate in cellular response to oxidative stress, likely in association with ERα in estrogen sensitive contexts, such as ER positive breast cancer subtypes.

2. Materials and methods

2.1. Yeast two-hybrid system

The cDNA region encoding the C-terminal part of human Che-1 (aa 470 to 558) was cloned into the pGBKT7 vector (Takara Bio Inc., Kusatsu, Shiga, Japan) in frame with the Gal4 DNA binding domain (pGBKT7-Che-1-C) and used as bait for yeast two-hybrid assay as previously described [51]. Bait interaction specificity was further analyzed cloning in pGBKT7 vector both the complete open reading frame of human Che-1 (pGBKT7-Che-1) and the Che-1 portion from aa 1 to aa 470 (pGBKT7- Che-1ΔC).

2.2. Cell cultures and treatments

HeLa human cervical cancer cells (ATCC, CCL-2) were grown in Dulbecco's modified Eagle's medium (DMEM) supplemented with 10 % foetal bovine serum (FBS), L-glutamine and penicillin/streptomycin (Thermo Fisher Scientific, Inc., Waltham, MA, USA). MCF-7 human breast cancer cells (ATCC, HTB-22) were grown in DMEM supplemented with 10 % heat-inactivated FBS, L-glutamine and penicillin/streptomycin. MCF10A breast epithelial cells (ATCC CRL-10317) were cultured in Ham's F-12 medium with 5 % horse serum, 0.5 mg/ml hydrocortisone, 10 mg/ml insulin, and 20 ng/ml EGF. All cell cultures were maintained at 37 °C in a humidified atmosphere of 5 % CO_2. Mycoplasma contamination was periodically checked by polymerase chain reaction (PCR) analysis.

Hydrogen peroxide (H_2O_2) was purchased from Merck & Co Inc. (Rahway, NJ USA). Oxidative stress was induced with daily fresh H_2O_2 solution prepared from stock solution 30 % (*w*/w) at concentrations and time indicated.

2.3. Transfection with siRNA and DNA constructs

Transfections were carried out using Lipofectin® Transfection Reagent and PLUS™ reagent or Lipofectamine 3000 reagents cells according to the manufacturer's instructions (Thermo Fisher Scientific Inc.). Cells were analyzed 48–72 h after transfection, and the efficiency of transfection and silencing was determined by RT-qPCR, immunoblotting, or immunofluorescence. siRNA-mediated interference experiments were performed using Stealth siRNA oligonucleotides (siAATF cat. no. 1299003 - HSS120157/HSS120158/HSS120159 and siCTRL cat. no. 12935300) (Thermo Fisher Scientific Inc.) and siSMART pool oligonucleotides (siHAX1 cat. no. M012168–01 and siCTRL cat. no. 001810–10) (Dharmacon Inc., Carlo Erba Reagents Srl, Cornaredo, MI, Italy). pCS2-MT-Che-1, pEGFP-HAX1 and pEGFP-HAX1 deletion mutants have been previously described [12,51].

2.4. Immunofluorescence

For endogenous proteins, cells were fixed in 3:7 methanol-acetone for 20 min at −20 °C, air dried and then preincubated in SM buffer (PBS containing 0.05 % saponin (Merck & Co Inc.) and 5 % BSA (Merck & Co Inc.) for 30 min at room temperature. Cells were then incubated overnight at 4 °C with the appropriate primary antibodies diluted in SM buffer. Cells were washed three times with PBS and incubated with secondary antibody for 45 min in SM buffer at room temperature. Cells transiently transfected with the indicated constructs were fixed 24 h after transfection with 4 % paraformaldehyde solution (Merck & Co Inc.) for 10 min at room temperature and then permeabilized with 0.2 % IgepalCA 630 (Merck & Co Inc.) for 10 min at room temperature. To label mitochondria, cells were incubated with 250 nM of MitoTracker® Red CMXRos M7512 (Thermo Fisher Scientific, Inc.) according to the manufacturer's instructions before fixation. Slides were mounted with ProLong™ Diamond Antifade Mountant with DAPI (Thermo Fisher Scientific, Inc.). Slides were examined by conventional epifluorescence microscopy (Olympus BX51). Images were captured using a digital camera SPOT RT3 and merged using the IAS2000 software. Information on the antibodies is listed in Supplementary Table S2.

2.5. Cell lysis and sub-cellular fractionation

Whole-cell extracts were prepared incubating the cells on ice for 10 min with Lysis buffer (50 mM Tris-HCl pH 7.5, 250 mM NaCl, 5 mM EDTA pH 8, 50 mM NaF, 0.1 mM Na_3VO_4, 0.1 % Triton X-100, 5 % glycerol) supplemented with a proteinase inhibitor cocktail (Merck & Co Inc.). Lysates were centrifuged at 12000*g* for 10 min at 4 °C and

supernatants collected. The mitochondrial enriched fraction was obtained by the Qproteome Mitochondria Isolation Kit (QIAGEN Hilden, Germany) according to the manufacturer's instructions. The heavy membrane (HM) enriched fraction was obtained as previously described [50]. The nuclei extracts were prepared from HeLa cells as previously described [60].

2.6. Co-immunoprecipitation and Western blotting

After protein extraction as described above, co-immunoprecipitations were performed. An equal amount of proteins (either whole-cell extract or mitochondria/heavy membrane enriched cell extract), was diluted in a 2:1 ratio between Lysis Buffer and Dilution buffer (50 mM Tris-HCl pH 7.5, 50 mM NaCl, 50 mM NaF, 0.1 mM Na_3VO_4, 15 % glycerol). Then, the diluted cell extract was pre-cleared with protein A/G PLUS-Agarose beads (Santa Cruz Biotechnology, Santa Cruz, CA, USA). Immunoprecipitation assays were performed overnight at 4 °C with 2 to 4 μg of indicated antibodies, previously bound to A/G PLUS- Agarose beads. Normal mouse IgG, "no-antibody", or "unrelated antibody" immunoprecipitations were performed as a negative control. Protein-bound beads were recovered by centrifugation and washed three times with the Wash buffer (1 Lysis buffer: 1 Dilution buffer) and once in PBS buffer. Immunoprecipitated proteins were eluted from beads by heating samples at 70 °C in LDS Sample Buffer for 10 min, followed by electrophoresis on 4–12 % NuPAGE ® Bis-Tris Gel System (Thermo Fisher Scientific, Inc.). Western blotting analysis of protein samples was carried out by standard procedures and signals were visualized by chemiluminescence ECL™ Select Western Blotting Detection Reagent (Cytiva, Marlborough, MA, USA) according to the manufacturer's instructions. Information on the antibodies is listed in Supplementary Table S2.

2.7. Cell viability assay

Cell viability was determined by MTT reduction assay. MCF-7 cells were plated at a density of 8×10^3 cells/well in octuplicate on 96-well plate and transfected the day after with the indicated constructs. 24 h after transfection cells were exposed to H_2O_2 at various concentrations (0 control, 0.25 mM, 0.5 mM, 1 mM) for 16 h. The culture medium was discarded, and cells were incubated with MTT (0.5 mg/ml in PBS; 100 μl/well) (Thermo Fisher Scientific, Inc.) at 37 °C for 4 h. Then, MTT was removed and 100 μl of DMSO (Merck & Co Inc.) was added to each well to dissolve the purple formazan crystals. Lastly, 570 nm absorbance values against 620 nm absorbance were calculated from the automated microplate reader (Bio-Rad Laboratories, Inc. Hercules, CA, USA).

2.8. Mitochondrial superoxide detection

Mitochondrial superoxide generation was detected using MitoSOX™ Red (Thermo Fisher Scientific, Inc.), a specific mitochondrial superoxide indicator of reactive oxygen species (ROS), according to manufacturer protocol. MitoSOX fluorescence analysis was performed as previously described [60].

2.9. Padlock assay

Phosphorylation of the padlock probe and Padlock assays were performed as previously described [12,61]. The Padlock probe sequences are presented in Supplementary Table S1.

2.10. RNA extraction, retrotranscription and quantitative real-time PCR (qPCR)

RNA was isolated using TRIzol® reagent (Thermo Fisher Scientific, Inc.) and was then reverse transcribed using a HighCapacity cDNA Reverse Transcription kit (Thermo Fisher Scientific, Inc.). Quantitative

real-time PCR assays were performed using the Fast SYBR™ Green Master Mix (Thermo Fisher Scientific, Inc.) in a StepOnePlus™ Real-Time PCR System according to the manufacturer's protocol. GAPDH was used for the normalization of mRNA and relative expression was calculated using the comparative Ct methods ($2- ^{\Delta\Delta Ct}$). Primers are presented in Supplementary Table S1.

2.11. Statistics

All experiments were repeated at least three times. Data are presented as means ± SD, when indicated. Two-tailed Student's *t*-tests with Benjamini–Hochberg correction were performed to compare one parameter between two groups. Statistical significance is indicated by asterisks as follows: *$P < 0.05$, **$P < 0.01$, ***$P < 0.001$, n.s. not significant. Microscopy images shown in the paper correspond to the most representative experiments.

3. Results

3.1. HAX1 interacts with Che-1

To detect candidate proteins that interact with Che-1/AATF, yeast two-hybrid (Y2H) assays were performed. A cDNA fragment encoding the C-terminal 88 amino acid residues of Che-1 (Che-1-C) (Fig. 1A), highly conserved among eucaryotes [62], was fused in-frame with the yeast Gal4 DNA binding domain in the vector pGBKT7 and used to screen a two-hybrid cDNA library prepared from human adult brain [51]. Several clones were isolated and the clone encoding for the HCLS1 Associated Protein X-1 (HAX1) was selected for further studies. The specificity of the Che-1/HAX1 interaction was confirmed in a two-hybrid assay co-transforming HAX1 with either Che-1-C or pGBKT7 constructs containing full-length Che-1 or Che-1 lacking the C-terminal region (Che-1-ΔC) (Fig. 1A). Both Che-1 and Che-1-C bound HAX1 whereas Che-1- ΔC did not interact with HAX1 protein (Fig. 1A). With the intent to define HAX1/Che-1 interaction in mammalian cells we performed a series of assays in different human cell lines: HeLa (cervical cancer cells), MCF-7 (breast cancer cells) and MCF10A (non-malignant breast epithelial cells). Immunofluorescence assays performed in HeLa and MCF-7 cells showed consistent partial colocalization of HAX1 and Che-1 proteins with a major site in mitochondria (Fig. 1B and Supplementary Fig. S1A). To confirm the interaction between the two proteins in this district, mitochondrial enriched lysate obtained from HeLa cells was used in co-immunoprecipitation experiments. A clear interaction between HAX1 and Che-1 proteins is shown in Fig. 1C. Analogously, we demonstrated HAX1/Che-1 interaction in MCF-7 cells using heavy membrane cellular fraction (HM), highly enriched in mitochondria (Fig. 1D). We confirmed the interaction between HAX1 and Che-1 proteins by co-immunoprecipitation experiments also in the non-tumorigenic MCF10A breast epithelial cells (Supplementary Fig. S1B).

3.2. Characterization of HAX1/Che-1 interaction and effect of HAX1 deletion constructs

Next, we intended to determine the protein regions of HAX1 (isoform 001) (Fig. 2A) crucial for the interaction with Che-1. To this end, HeLa cells were transiently co-transfected with myc-Che-1 full-length and EGFP-HAX1 or EGFP-HAX1 deletion constructs (Fig. 2B). Then, whole cell extracts were immunoprecipitated with anti-myc tag antibody and analyzed by western blot. Fig. 2B and C show that the construct expressing the C terminal portion of HAX1 (179–279 aa) displays the highest binding affinity toward Che-1 protein, with two crucial interacting regions working in synergy, one region spanning from amino acids 179 to 190 and the other between amino acids 234 and 279. In parallel the same HAX1 mutants were characterized by immunofluorescence, and the two complementary mutants HAX1N-190 (1 aa-190 aa), mimicking HAX1-Kostmann mutant protein, and HAX1C-89 (190
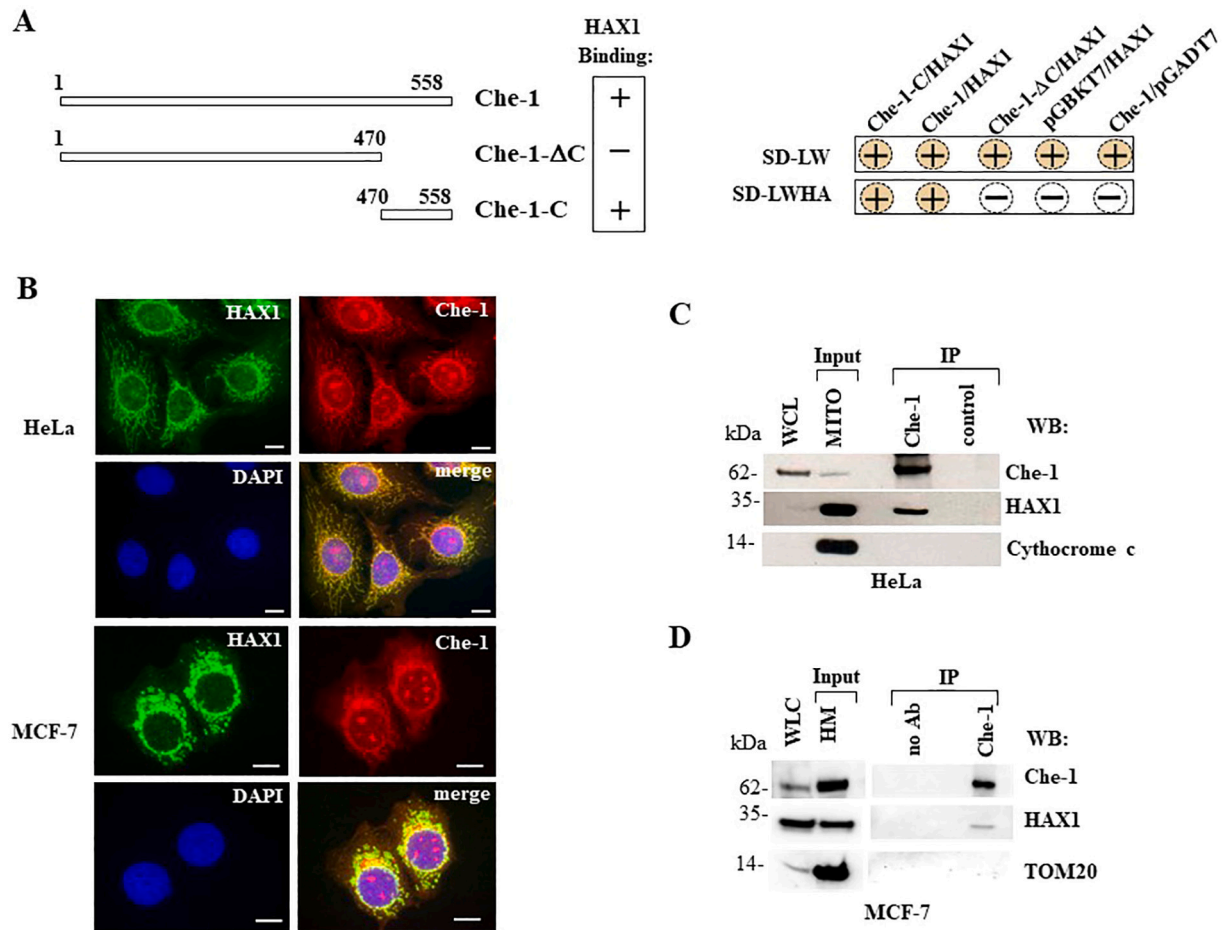
Fig. 1. Human Che-1 interacts with HAX1. A: Che-1 deletion mutants and full-length proteins were used as the bait for the yeast two-hybrid assay (left panel). Yeast transformed with the indicated constructs were plated onto SD media lacking leucine and tryptophan (-LW) to verify the expression of both bait (W+) and prey (L+) plasmids, or onto media lacking leucine, tryptophan, histidine and adenine (-LWHA) to examine the interaction between bait and prey proteins (right panel). B: Dual-label indirect immunofluorescence performed in HeLa cells (up) and MCF-7 cells (bottom) with the anti-Che-1 rat polyclonal antibody and the anti-HAX1 rabbit polyclonal antibody to visualize the immunolocalization of endogenous HAX1 (green) and Che-1 (red). Extensive colocalization (yellow) between HAX1 and Che-1 is visualized by the merged-colour image. Nuclei were stained with DAPI (blue). Scale bar, 50 μm. C: Mitochondria-enriched lysate (MITO) from HeLa cells was immunoprecipitated with rabbit polyclonal anti-Che-1 antibody or with control IgG. Immunoprecipitated samples were analyzed by western blot using the indicated antibodies. D: MCF-7 cells extract enriched in heavy membrane fraction (HM) was immunoprecipitated using anti-Che-1 rabbit polyclonal antibody or with no antibodies (no-Ab). Immunoprecipitation and co-immunoprecipitation were analyzed by western blot using the indicated antibodies. (For interpretation of the references to colour in this figure legend, the reader is referred to the web version of this article.)

aa-279 aa) together with HAX1C-55, do not maintain strictly mitochondrial localization (Supplementary Fig. S2A). Conversely, as shown in Fig. 2D and Supplementary Fig. S2A, the HAX1C-100 mutant with a high binding affinity to Che-1 maintains mainly mitochondrial localization. The high affinity of HAX1C-100 mutant to Che-1 binding, prompted us to investigate whether HAX1C-100 could play any role(s) in interfering with HAX1/Che-1 protein interaction. As shown in Fig. 2E, increased expression of EGFP-HAX1C-100 resulted in a marked decrease of EGFP-HAX1 full length co-immunoprecipitated with myc-Che-1, quantified by densitometric analysis (Supplementary Fig. S2B). This result suggests that HAX1C-100 mutant acts as a dominant negative by inhibiting HAX1/Che-1 interaction. To elucidate HAX1C-100 mutant dominant negative properties upon oxidative stress, we measured cellular viability in MCF-7 cells transfected with EGFP (control), EGFP-HAX1 and EGFP-HAX1C-100 respectively, treated with increasing concentrations of H_2O_2 for 16 h. Cell viability following H_2O_2 treatment was assessed by 3-(4,5-dimethylthiazol-2-yl)-2,5-diphenyltetrazolium bromide (MTT) assay. As shown in Fig. 2F, cells transfected with EGFP-HAX1, compared to cells transfected with EGFP, display in response to oxidative stress a clear increase in viability related to the anti-apoptotic role of HAX1, as expected. The viability of cells transfected with EGFP-

HAX1C-100 goes in the opposite trend. We suppose that HAX1C-100 acts as effective dominant negative mutant by competing with the interaction of endogenous Che-1 and HAX1 proteins and counteracting their anti-apoptotic effect [28,42,43].

3.3. The association of HAX1 and Che-1 proteins is strengthened by oxidative stimuli

Then, we examined HAX1 and Che-1 endogenous proteins both individually and in association under oxidative stress conditions, induced by H_2O_2 treatment (1 mM, 3 h), at concentration described to induce ROS activation [28] (Supplementary Fig. S3A, B). First, we compared by immunofluorescence assays in HeLa and MCF-7 cells the subcellular localization of HAX1 and Che-1 proteins before and after H_2O_2 treatment (Fig. 3A and Supplementary Fig. S4B). In the absence of stress condition, HAX1 localized primarily within the mitochondria and Che-1 in nucleus/nucleolus and mitochondria. Upon H_2O_2 treatment, we observed a clear alteration of the subcellular localization of both HAX1 and Che-1 proteins. Consistent with previous finding that reported HAX1 to be a nucleocytoplasmic shuttling protein after specific cellular stress [63], we detected a certain HAX1 nuclear accumulation
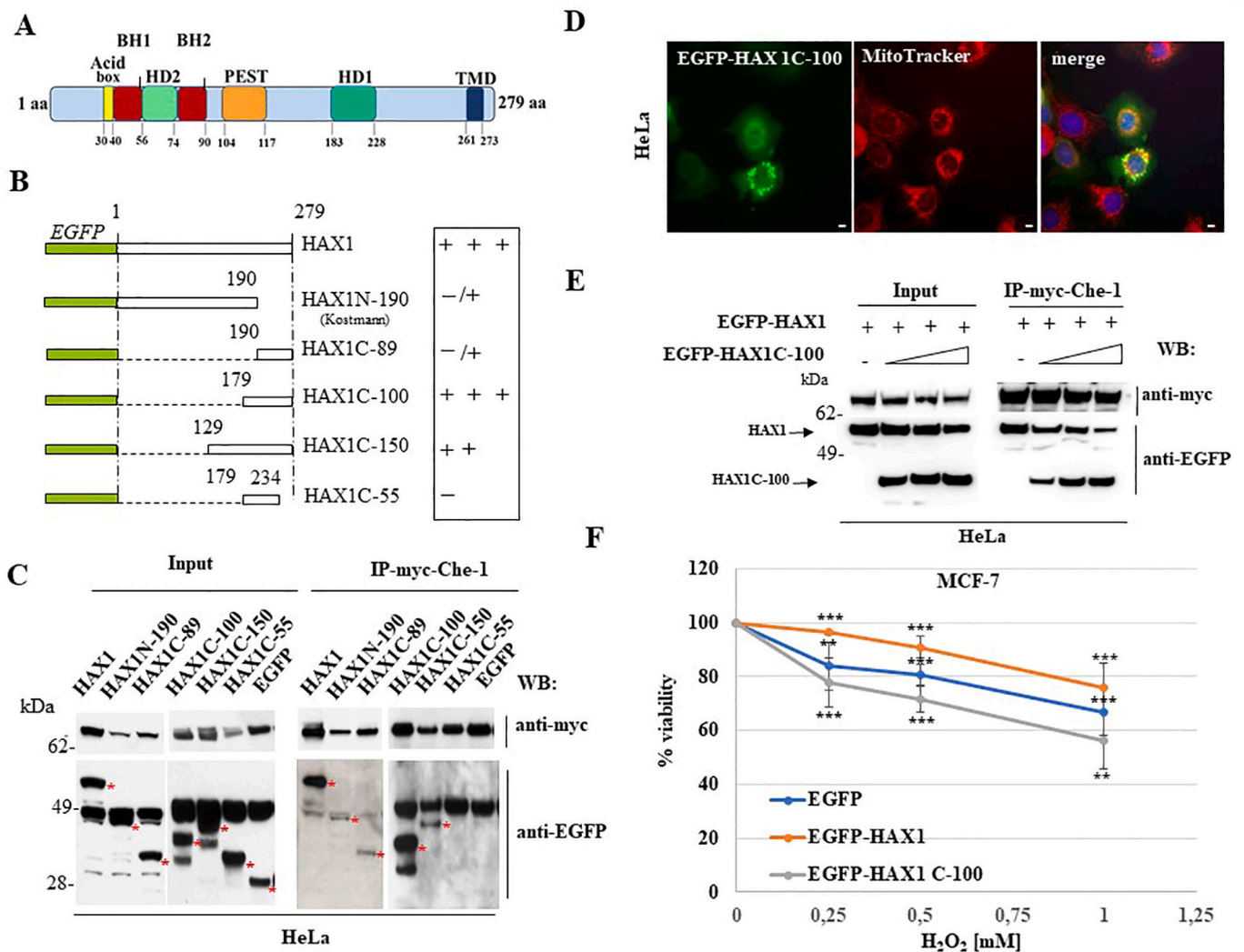
Fig. 2. Characterization of HAX1 regions that bind Che-1 protein and effect of HAX1C-100 deletion construct as dominant negative. A: Domain map of HAX1 protein. Acid box with the EE motif, BH1 and BH2 (Bcl-2 protein homology domains); HD1 and HD2 (HAX1 domains conserved among species); PEST domain and TMD (transmembrane-like domain) were indicated. B: Schematic representation of EGFP-HAX1 derived deletion constructs and their ability to bind Che-1 protein. C: Whole-cell extracts of HeLa cells transiently transfected with myc-Che-1 and EGFP-HAX1 or its deletion constructs were immunoprecipitated with anti-myc tag monoclonal antibody and analyzed by western blot using anti-EGFP monoclonal antibody (right panel). The total cell lysates (Input) were immunoblotted to verify the correct expression of the transfected molecules (left panel). The asterisks indicate the main bands. D: HeLa cells transfected with EGFP-HAX1C-100 were stained with mitochondrion-selective dye MitoTracker (red). Nuclei were stained with DAPI (blue). Scale bar, 50 μm. E: Competition between HAX1C-100 and HAX1 for binding to Che-1. The total protein extracts of HeLa cells transfected with myc-Che-1, EGFP-HAX1 and increasing amounts of EGFP-HAX1C-100 were immuno-precipitated with anti-myc tag monoclonal antibody and analyzed by western blot using anti-GFP monoclonal antibody. Arrows indicate HAX1 and HAX1C-100 bands. F: Cell viability following H_2O_2-induced oxidative stress. MCF-7 cells were transfected with EGFP, EGFP-HAX1, and EGFP-HAX1C-100 respectively and 24 h later treated with increasing concentrations of H_2O_2 (0.25 mM, 0.5 mM, 1 mM) for 16 h. The viability curve was performed by MTT assay. Data are reported as the mean ± SD of at least four independent experiments ($*p \leq 0.05$; $**p \leq 0.01$; $***p \leq 0.001$). (For interpretation of the references to colour in this figure legend, the reader is referred to the web version of this article.)

upon H_2O_2 treatment in our experimental conditions (Fig. 3A), supported by western blot analysis of nuclear fractions prepared from HeLa cells untreated and treated with H_2O_2 (Supplementary Fig. S4A). Concomitantly, we observed a significant loss of nucleolar Che-1 staining upon H_2O_2 treatment (Fig. 3A and Supplementary Fig. S4B). Co-immunostaining with nucleolin, a major component of nucleoli, underlined an independent mislocalization of Che-1 and nucleolin upon oxidative stress induction (Supplementary Fig. S4C). We then quantified by ImageJ analysis the colocalization between HAX1 and Che-1 before and after H_2O_2 treatment. As shown in Fig. 3B a reinforced colocalization between HAX1 and Che-1 was observed after H_2O_2 treatment. In agreement with these findings, by co-immunoprecipitation in MCF-7 cells, upon H_2O_2 stimulation, it was detected a consistent enhancement of HAX1/Che-1 interaction (Fig. 3C, D), concomitantly with a

small increase of HAX1 and Che-1 protein levels (Fig. 3E). These results underline the importance of HAX1/Che-1 interaction in cellular response to oxidative stress. Modulation of oxidative stress status in the cells is a risk factor associated with breast cancer. Previous reports have demonstrated that HAX1 is overexpressed in breast cancer and represents an independent risk factor for metastasis. Importantly, HAX1 was previously shown to directly bind ERα, a protein involved in breast cancer initiation and progression via an oxidative stress-mediated pathway [4,34,37,64,65]. We confirmed in MCF-7 cells the interaction of HAX1 with ERα by co-immunoprecipitation experiments (Fig. 3D). Remarkably, we observed that the HAX1/ERα association is also strengthened by oxidative stimuli.
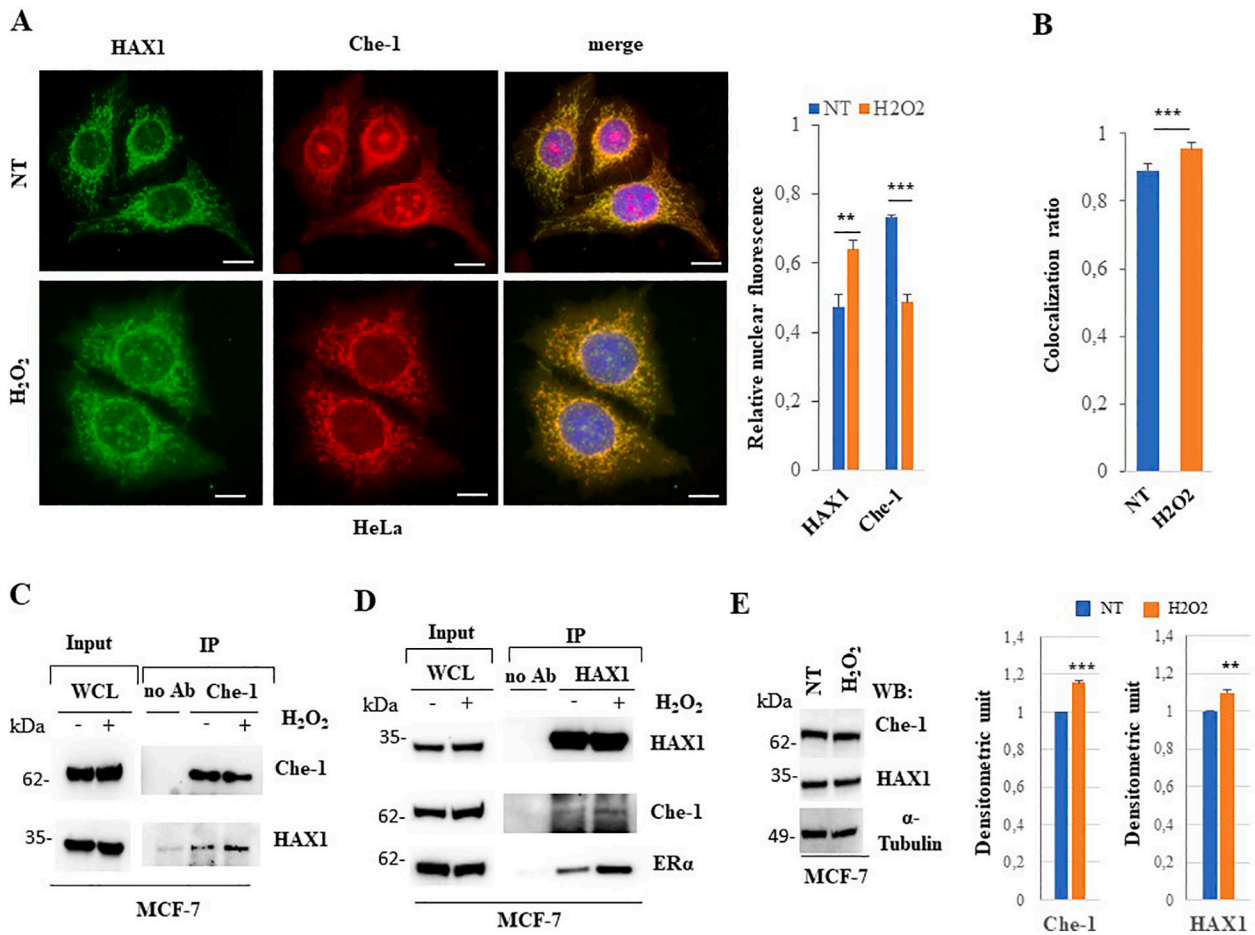
Fig. 3. The association of HAX1 and Che-1 proteins is strengthened by oxidative stimuli. A: Dual-label indirect immunofluorescence with anti-HAX1 rabbit poly-clonal antibody (green) and the anti-Che-1 rat polyclonal antibody (red) in HeLa cells untreated (NT) or treated with H_2O_2 (1 mM, 3 h). Nuclei are stained with DAPI (blue). Scale bar, 50 μm (left panel). Pearson correlation coefficient of relative nuclear localization of HAX1 and Che-1 in cells untreated or treated with H_2O_2 (1 mM, 3 h) shown in the histogram was calculated by ImageJ Coloc 2. At least 25 fields by three different experiments were analyzed, and the data were shown as mean ± S·D ($*p \leq 0.05$; $**p \leq 0.01$; $***p \leq 0.001$, Student's *t*-test) (right panel). B: Histograms represent the Pearson correlation coefficient of HAX1/Che-1 total coloc-alization ratio in cells untreated or treated with H_2O_2 (1 mM, 3 h), calculated by ImageJ JACoP. At least 15 fields by three different experiments were analyzed, and the data were shown as mean ± S.D. ($*p \leq 0.05$; $**p \leq 0.01$; $***p \leq 0.001$, Student's t-test). C: Cell lysates prepared from MCF-7 cells untreated or treated with H_2O_2 (1 mM, 3 h) were immunoprecipitated with anti-Che-1 monoclonal antibody and analyzed by western blotting. Used antibodies are indicated. D: Whole cell lysates prepared from MCF-7 cells untreated or treated with H_2O_2 (1 mM, 3 h) were immunoprecipitated with anti-HAX1 polyclonal antibody and analyzed by western blotting. Used antibodies are indicated. E: Representative western blot of MCF-7 cells untreated (NT) or treated with H_2O_2 (1 mM, 3 h). The antibodies used are indicated (left panel). Densitometric analyses of Che-1 and HAX1 protein levels represents the mean ± S.D. of five independent experiments ($*p \leq 0.05$; $**p \leq 0.01$; $***p \leq 0.001$) (right panel). (For interpretation of the references to colour in this figure legend, the reader is referred to the web version of this article.)

3.4. Knockdown of Che-1 induces downregulation and altered cellular distribution of HAX1

To further clarify the significance of HAX1/Che-1 interaction in steady state condition and upon oxidative stress, we performed RNAi-mediated knockdown studies with or without oxidative stress induc-tion. Taking into account that HAX1 and Che-1 proteins are key regu-lators of apoptosis, MCF-7 cells were transiently transfected with either Che-1 or HAX1 siRNAs and then treated or not with H_2O_2. Significantly, in accordance with previous observations [52,54,59], we found that Che-1 silencing induces a significant increase of mitochondrial reactive oxygen species (ROS) and this phenomenon is exacerbated when Che-1 silencing is combined with H_2O_2 treatment (Fig. 4A). Concomitantly, we demonstrated by quantitative real time RT-PCR (qPCR) analysis that Che-1 knockdown specifically reduces the HAX1 mRNA levels of about 50 % in steady state condition, and this reduction is not substantially affected when Che-1 silencing is combined to H_2O_2 treatment (Fig. 4B and Supplementary Fig. S5A). The effect of Che-1 knockdown on HAX1 mRNA levels in steady state condition was also confirmed by padlock

experiments that allowed sensitive detection of HAX1 endogenous mRNAs (Fig. 4C).

Next, we evaluated the effects on HAX1 protein levels following Che-1 silencing in MCF-7 cells, treated or not with H_2O_2. As shown in Fig. 5A, western blot analysis revealed that Che-1 knockdown induces a decrease of HAX1 protein levels coherent with the HAX1 mRNA decrease in un-treated cells (Fig. 5A). The effect of Che-1 knockdown on HAX1 protein level/localization was explored also by immunofluorescence experi-ments following Che-1 silencing, in MCF-7 untreated and treated with H_2O_2. Fig. 5B shows, upon Che-1 silencing, a general decrease of HAX1 protein staining coupled with an increased HAX1 presence in nuclear discrete dots that don't colocalize with nucleolin protein (Supplemen-tary Fig. S6A). The HAX1 downregulation induced by Che-1 knockdown appears not affected by oxidative stress induction with H_2O_2 treatment, in our experimental conditions. These data indicate that Che-1 depletion induces per se downregulation and altered cellular distribution of HAX1.

In contrast, HAX1 silencing in our experimental conditions induces only a slight decrease of Che-1 mRNA levels both in untreated and H_2O_2 treated MCF-7 cells (Supplementary Fig. S5B, C). Accordingly, Che-1
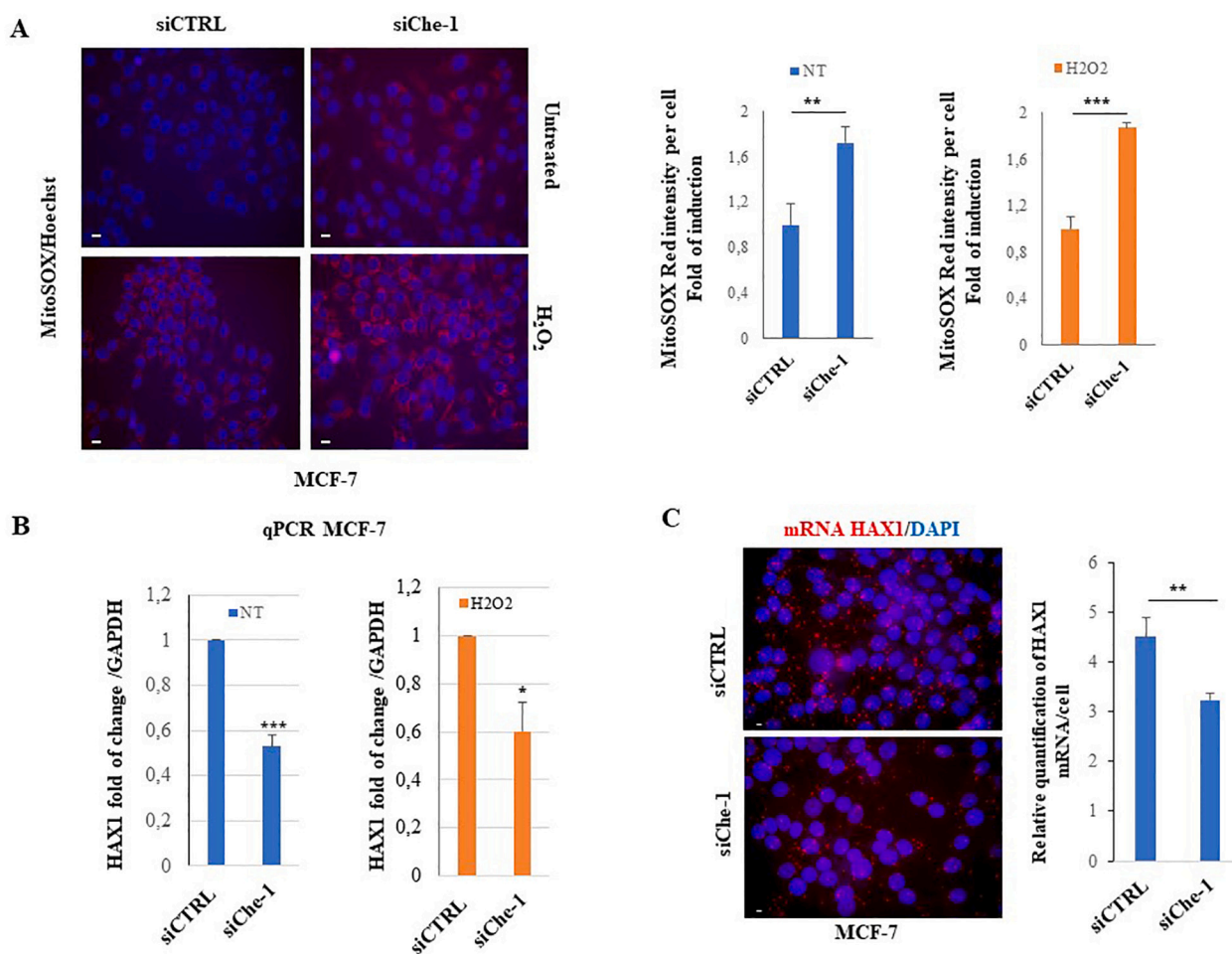
Fig. 4. Effect of Che-1 knockdown on HAX1 mRNA with or without oxidative stress induction. A: Representative fluorescence images of MCF-7 cells upon Che-1 silencing (siCTRL, siChe-1), untreated (NT) or treated with H_2O_2 (1 mM, 3 h). The cellular level of superoxide was visualized by the MitoSOX (red) mitochondrial Superoxide Indicator staining. Nuclei were stained with Hoechst (blue). Scale bar, 50 μm. Histogram reporting fold of increase of MitoSOX fluorescence in MCF-7 cells upon Che-1 silencing alone or combined with of H_2O_2 treatment (1 mM, 3 h) (*$p \leq 0.05$; **$p \leq 0.01$; ***$p \leq 0.001$ vs. the siCTRL). B: Quantitative real time RT-PCR (qPCR) analysis of HAX1 mRNA in MCF-7 cells upon Che-1-silencing (siCTRL, siChe-1), untreated (NT) or treated with H_2O_2 (1 mM, 3 h). The gene expression ratio of HAX1 mRNA, normalized as indicated, is shown as the mean ± SD from at least four independent experiments performed in triplicate (*$p \leq 0.05$; **$p \leq 0.01$; ***$p \leq 0.001$ vs. the siCTRL). C: Visualization of HAX1 mRNA (red dots) upon Che-1-silencing in MCF-7 cells (siCTRL, siChe-1) by padlock probe-based exponential rolling circle amplification. Nuclei were stained with DAPI (blue). Scale bar, 50 μm. Histogram of HAX1 mRNA amplicons per cell detected (left). Data represents the mean ± S.D. of at least three independent experiments (*$p \leq 0.05$; **$p \leq 0.01$; ***$p \leq 0.001$ vs. the siCTRL). (For interpretation of the references to colour in this figure legend, the reader is referred to the web version of this article.)

protein levels analyzed in steady state condition appear not significantly altered upon HAX1 knockdown (Supplementary Fig. S5D).

All together these results suggest an involvement of Che-1 in the regulation of HAX1 not strictly dependent on oxidative stress induction.

4. Discussion

Although HAX1 protein is implicated in many cellular processes, its molecular mechanisms of action remain elusive. We have previously shown that HAX1 interacts with the psoriasis candidate Coiled-Coil alpha-Helical Rod 1 (CCHCR1) protein and it may influence fate and stability of specific transcripts via protein/protein interaction [12]. In the present study, we provide new insights into the biological role of the HAX1 protein, by showing that HAX1 is a new Che-1/AATF interaction partner and notably their interaction is strengthened after oxidative stress stimuli. We have shown that HAX1 binds to the C-terminal region of Che-1 and colocalize with Che-1 mainly at mitochondrial level. Previous studies indicated that HAX1, due to its intrinsically disordered structure, interacts in a versatile way with a wide spectrum of proteins, that vary in different cellular and localization contexts [17,66]. We

revealed the presence of HAX1 and Che-1 in the same immune-complex in the whole cell extract and in the heavy membrane/mitochondria enriched fractions in different human cell lines, as HeLa derived from cervical carcinoma, MCF-7 derived from breast cancer cells and MFC10A used as a model for normal mammary epithelial cells. To understand more fully the nature of the HAX1/Che-1 interaction, we defined the regions of HAX1 protein critical for Che-1 binding, using HAX1 deletion constructs. Significantly, HAX1 C-terminal region spanning the last 100aa (HAX1C-100), including the transmembrane domain with a conserved α-helix motif crucial for protein-protein interaction [17,28], is responsible for Che-1 interaction. The HAX1C-100 construct maintains mainly mitochondrial localization and it shows the highest binding affinity to Che-1. Importantly, our data indicate that HAX1C-100 acts as dominant negative mutant by competing with the interaction of endogenous Che-1 and HAX1 proteins and counteracting their anti-apoptotic effect [28,42,43]. Since HAX1 is involved in the antagonism of apoptotic processes in cellular response to oxidative stress [10,17,28] and Che-1 as well participates in cellular response to different types of stresses [42–45,52,54,55,67,68], we examined whether HAX1 and Che-1 individually and in association were regulated
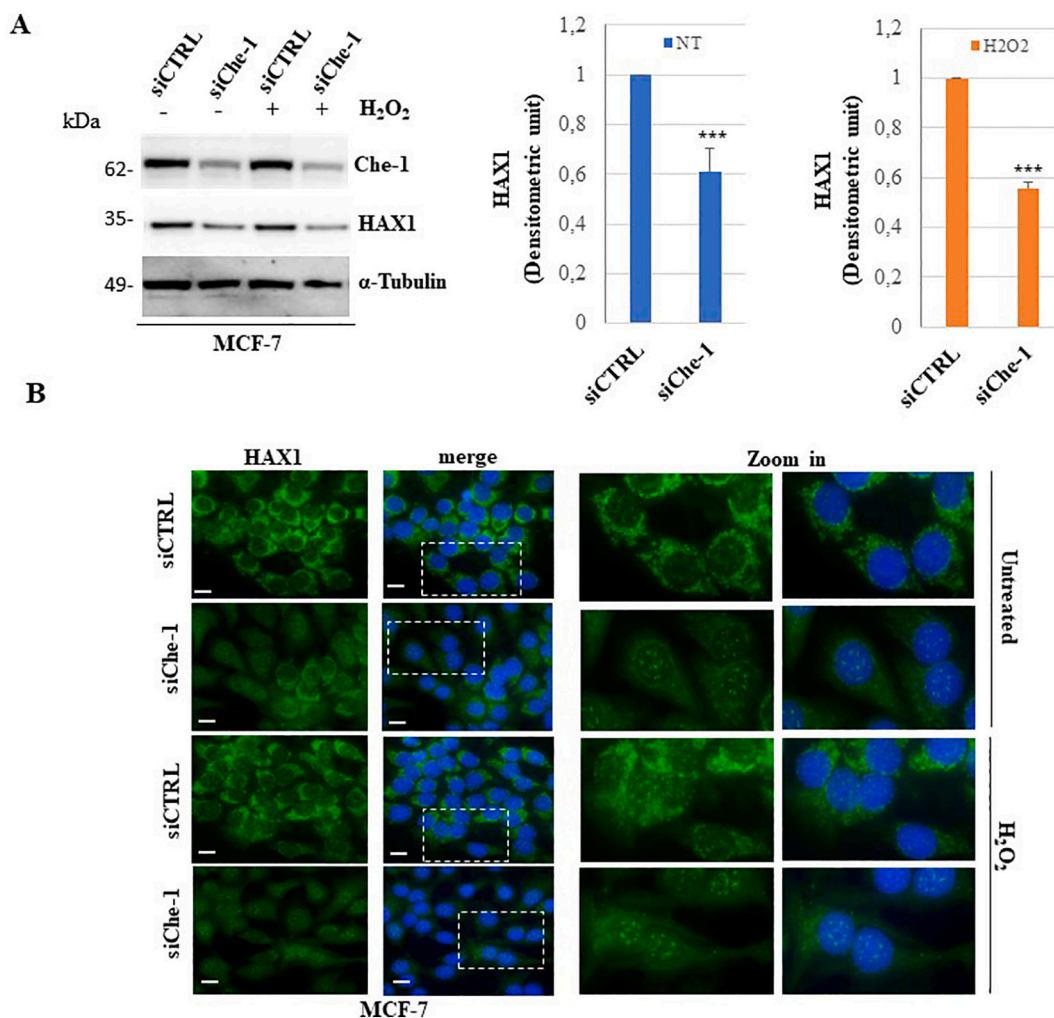
Fig. 5. Effect of Che-1 knockdown on HAX1 protein with or without oxidative stress induction. A: Representative western blot of MCF-7 cells upon Che-1-silencing (siCTRL, siChe-1), untreated or treated with H_2O_2 (1 mM, 3 h). The antibodies used are indicated. Densitometric analysis represents the mean ± S.D. of at least four independent experiments (right panel). B: Representative fluorescence images of MCF-7 cells upon Che-1-silencing (siCTRL, siChe-1), untreated or treated with H_2O_2 (1 mM, 3 h). Indirect immunofluorescence was performed with the anti-HAX1 rabbit polyclonal antibody (green). Nuclei were stained with DAPI (blue). Scale bar, 50 μm. (For interpretation of the references to colour in this figure legend, the reader is referred to the web version of this article.)

under oxidative stress conditions. We observed an altered subcellular localization of both HAX1 and Che-1 proteins upon H_2O_2 treatment, with an increase of HAX1 in the nucleus and a decrease of Che-1 in the nucleolus. The Che-1 shuttling between the nucleolus and nucleoplasm in response to oxidative stress conditions is in accordance with the recent evidence that Che-1 is essential in ribosome biogenesis and with the emerging role of nucleoli in cellular stress response [40,45,46,69–71]. Anyway, we observed and independent mislocalization of Che-1 and nucleolin upon H_2O_2 treatment, indicating for Che-1 an individual fate, that is not merely a consequence of stress-related rearrangement of nucleolar compartment. Furthermore, we showed that HAX1/Che-1 colocalization is significantly reinforced after H_2O_2 treatment. Significantly, the increased percentage of colocalization between the two proteins correlates with their strengthened interaction upon oxidative stress induction. These results underline the importance of HAX1/Che-1 interaction in cellular response to oxidative stress. Oxidative stress plays an important role in both initiation and progression of breast cancer. Both HAX1 and Che-1 are crucial targets in the field of cancer research on account of their involvement in regulation of apoptosis and cell survival. Importantly HAX1 regulates cell migration, a key process in carcinogenesis and metastasis [7]. Of note, both HAX1 and Che-1 have been shown by other research groups to directly bind ERα, a protein involved in breast cancer initiation and progression via an

oxidative stress-mediated pathway [4,34,37,64,65,72,73]. We report for the first time that the interaction of HAX1 with ERα is strengthened by oxidative stimuli. Moreover, we demonstrated that Che-1 depletion correlates with HAX1 downregulation and altered cellular distribution, regardless of oxidative stress. In this perspective, HAX1 could contribute to antiapoptotic activity exerted by Che-1, acting as Che-1 downstream gene. Our findings on HAX1/Che-1 interaction provide insights into the molecular mechanisms underlying their antiapoptotic activity in both physiological and pathological conditions. Importantly, HAX1, Che-1 and ERα have been independently shown to be RNA binding proteins [11,45,74], this common ability allows to speculate that at least part of their functions can be exerted through the control of specific RNA metabolism, upon specific stresses. It is possible to hypothesize that these three proteins may bind and regulate single transcripts or group of transcripts in shared pathways. In MCF-7 cells, our preliminary mRNA level analysis of cyclin D1, a key ERα target [75], suggests a transcription-independent activity of ERα after 3 h of H_2O_2 treatment (data not shown). Further studies are needed to define the potential coordinated activity of HAX1, Che-1 and ERα in cellular stress response pathways involved in breast cancer progression, pointing to the use of these molecules as biomarkers and effective therapeutic targets.

Supplementary data to this article can be found online at https://doi.org/10.1016/j.bbamcr.2023.119587.

Funding

CRediT authorship contribution statement

Cinzia Pisani: Investigation, Conceptualization, Formal analysis, Writing – original draft. **Annalisa Onori:** Investigation, Methodology, Data curation. **Francesca Gabanella:** Methodology, Formal analysis, Data curation. **Simona Iezzi:** Methodology, Investigation, Writing – review & editing. **Roberta De Angelis:** Methodology. **Maurizio Fanciulli:** Resources, Writing – review & editing. **Andrea Colizza:** Resources, Writing – review & editing. **Marco de Vincentiis:** Resources, Writing – review & editing. **Maria Grazia Di Certo:** Investigation, Writing – review & editing. **Claudio Passananti:** Conceptualization, Investigation, Supervision, Funding acquisition, Writing – original draft. **Nicoletta Corbi:** Conceptualization, Investigation, Supervision, Funding acquisition, Writing – original draft.

Declaration of competing interest

The authors declare that they have no known competing financial interests or personal relationships that could have appeared to influence the work reported in this paper.

Data availability

The data presented in this study are available on request from the corresponding author.

Acknowledgments

References

[1] Y. Suzuki, C. Demoliere, D. Kitamura, H. Takeshita, U. Deuschle, T. Watanabe, HAX-1, a novel intracellular protein, localized on mitochondria, directly associates with HS1, a substrate of Src family tyrosine kinases, J. Immunol. 158 (1997) 2736–2744.

[2] A. Trebinska, A. Rembiszewska, K. Ciosek, K. Ptaszynski, S. Rowinski, J. Kupryjanczyk, et al., HAX-1 overexpression, splicing and cellular localization in tumors, BMC Cancer 10 (2010) 76.

[3] Z. Liang, Y. Zhong, L. Meng, Y. Chen, Y. Liu, A. Wu, et al., HAX1 enhances the survival and metastasis of non-small cell lung cancer through the AKT/mTOR and MDM2/p53 signaling pathway, Thorac. Cancer 11 (2020) 3155–3167.

[4] A. Trebinska-Stryjewska, L. Szafron, A. Rembiszewska, M. Wakula, S. Tabor, R. Sienkiewicz, et al., Cytoplasmic HAX1 is an independent risk factor for breast cancer metastasis, J. Oncol. 2019 (2019) 6375025.

[5] X. Li, T. Li, B. You, Y. Shan, S. Shi, X. Cao, et al., Expression and function of HAX-1 in human cutaneous squamous cell carcinoma, J. Cancer 6 (2015) 351–359.

[6] V. Radhika, D. Onesime, J.H. Ha, N. Dhanasekaran, Galpha13 stimulates cell migration through cortactin-interacting protein Hax-1, J. Biol. Chem. 279 (2004) 49406–49413.

[7] A. Balcerak, A. Trebinska-Stryjewska, M. Wakula, M. Chmielarczyk, U. Smietanka, T. Rubel, et al., HAX1 impact on collective cell migration, cell adhesion, and cell shape is linked to the regulation of actomyosin contractility, Mol. Biol. Cell 30 (2019) 3024–3036.

[8] A.G. Ramsay, M.D. Keppler, M. Jazayeri, G.J. Thomas, M. Parsons, S. Violette, et al., HS1-associated protein X-1 regulates carcinoma cell migration and invasion via clathrin-mediated endocytosis of integrin alphavbeta6, Cancer Res. 67 (2007) 5275–5284.

[9] Y.L. Hu, Y. Feng, P. Ma, F. Wang, H. Huang, Y.B. Guo, et al., HAX-1 promotes the migration and invasion of hepatocellular carcinoma cells through the induction of epithelial-mesenchymal transition via the NF-κB pathway, Exp. Cell Res. 381 (2019) 66–76.

[10] Y.L. Li, W.F. Cai, L. Wang, G.S. Liu, C. Paul, L. Jiang, et al., Identification of the functional autophagy-regulatory domain in HCLS1-associated protein X-1 that resists against oxidative stress, DNA Cell Biol. 37 (2018) 432–441.

[11] A. Balcerak, E. Macech-Klicka, M. Wakula, R. Tomecki, K. Goryca, M. Rydzanicz, et al., The RNA-binding landscape of HAX1 protein indicates its involvement in translation and ribosome assembly, Cells. 11 (2022).

[12] C. Pisani, A. Onori, F. Gabanella, M.G. Di Certo, C. Passananti, N. Corbi, Identification of protein/mRNA network involving the PSORS1 locus gene CCHCR1 and the PSORS4 locus gene HAX1, Exp. Cell Res. 399 (2021) 112471.

[13] M. Al-Maghrebi, H. Brule, M. Padkina, C. Allen, W.M. Holmes, Z.E. Zehner, The 3′ untranslated region of human vimentin mRNA interacts with protein complexes containing eEF-1gamma and HAX-1, Nucleic Acids Res. 30 (2002) 5017–5028.

[14] E. Sarnowska, E.A. Grzybowska, K. Sobczak, R. Konopinski, A. Wilczynska, M. Szwarc, et al., Hairpin structure within the 3′UTR of DNA polymerase beta mRNA acts as a post-transcriptional regulatory element and interacts with Hax-1, Nucleic Acids Res. 35 (2007) 5499–5510.

[15] Y. Fan, M. Murgia, M.I. Linder, Y. Mizoguchi, C. Wang, M. Łyszkiewicz, et al., HAX1-dependent control of mitochondrial proteostasis governs neutrophil granulocyte differentiation, J. Clin. Invest. 132 (2022).

[16] C. Klein, Kostmann's disease and HCLS1-associated protein X-1 (HAX1), J. Clin. Immunol. 37 (2017) 117–122.

[17] M. Wakula, A. Balcerak, T. Rubel, M. Chmielarczyk, R. Konopinski, F. Lyczek, et al., The interactome of multifunctional HAX1 protein suggests its role in the regulation of energy metabolism, de-aggregation, cytoskeleton organization and RNA-processing, Biosci. Rep. 40 (2020), BSR20203094.

[18] S.V. Yap, E. Vafiadaki, J. Strong, A. Kontrogianni-Konstantopoulos, HAX-1: a multifaceted antiapoptotic protein localizing in the mitochondria and the sarcoplasmic reticulum of striated muscle cells, J. Mol. Cell. Cardiol. 48 (2010) 1266–1279.

[19] X.B. Guo, X. Deng, Y. Wei, Hematopoietic substrate-1-associated protein X-1 regulates the proliferation and apoptosis of endothelial progenitor cells through Akt pathway modulation, Stem Cells 36 (2018) 406–419.

[20] M. Szwarc, E. Sarnowska, E.A. Grzybowska, HAX-1 protein: multifunctional factor involved in apoptosis, cell migration, endocytosis and mRNA transport, Postepy Biochem. 53 (2007) 218–227.

[21] J. Yan, C. Ma, J. Cheng, Z. Li, C. Liu, HAX-1 inhibits apoptosis in prostate cancer through the suppression of caspase-9 activation, Oncol. Rep. 34 (2015) 2776–2781.

[22] J.R. Chao, E. Parganas, K. Boyd, C.Y. Hong, J.T. Opferman, J.N. Ihle, Hax1-mediated processing of HtrA2 by Parl allows survival of lymphocytes and neurons, Nature. 452 (2008) 98–102.

[23] Y. Han, Y.S. Chen, Z. Liu, N. Bodyak, D. Rigor, E. Bisping, et al., Overexpression of HAX-1 protects cardiac myocytes from apoptosis through caspase-9 inhibition, Circ. Res. 99 (2006) 415–423.

[24] J. Shaw, L.A. Kirshenbaum, HAX-1 represses postmitochondrial caspase-9 activation and cell death during hypoxia-reoxygenation, Circ. Res. 99 (2006) 336–338.

[25] W.B. Li, J. Feng, S.M. Geng, P.Y. Zhang, X.N. Yan, G. Hu, et al., Induction of apoptosis by Hax-1 siRNA in melanoma cells, Cell Biol. Int. 33 (2009) 548–554.

[26] X. Luo, Z. Li, X. Li, G. Wang, W. Liu, S. Dong, et al., hSav1 interacts with HAX1 and attenuates its anti-apoptotic effects in MCF-7 breast cancer cells, Int. J. Mol. Med. 28 (2011) 349–355.

[27] X. Deng, L. Song, W. Zhao, Y. Wei, X.B. Guo, HAX-1 protects glioblastoma cells from apoptosis through the Akt1 pathway, Front. Cell. Neurosci. 11 (2017) 420.

[28] Q. Dong, D. Li, H. Zhao, X. Zhang, Y. Liu, Y. Hu, et al., Anti-apoptotic HAX-1 suppresses cell apoptosis by promoting c-Abl kinase-involved ROS clearance, Cell Death Dis. 13 (2022) 298.

[29] B. Fadeel, E. Grzybowska, HAX-1: a multifunctional protein with emerging roles in human disease, Biochim. Biophys. Acta 2009 (1790) 1139–1148.

[30] X. Li, J. Jiang, R. Yang, X. Xu, F. Hu, A. Liu, et al., Expression of HAX-1 in colorectal cancer and its role in cancer cell growth, Mol. Med. Rep. 12 (2015) 4071–4078.

[31] F. Huang, X. Wu, M. Wei, H. Guo, H. Li, Z. Shao, et al., miR-654-5p targets HAX-1 to regulate the malignancy behaviors of colorectal cancer cells, Biomed. Res. Int. 2020 (2020), 4914707.

[32] Y.J. Wu, Z.Q. Cai, R.M. He, X.C. Wang, L.L. Cong, F.H. Qiu, Knockdown of long noncoding RNA 01124 inhibits the malignant behaviors of colon cancer cells via miR-654-5p/HAX-1, Evid. Based Complement. Alternat. Med. 2022 (2022) 1092107.

[33] C. Sheng, Q. Ni, Expression of HAX1 and Ki-67 in breast cancer and its correlations with patient's clinicopathological characteristics and prognosis, Int. J. Clin. Exp. Med. 8 (2015) 20904–20910.

[34] K. Kasashima, E. Ohta, Y. Kagawa, H. Endo, Mitochondrial functions and estrogen receptor-dependent nuclear translocation of pleiotropic human prohibitin 2, J. Biol. Chem. 281 (2006) 36401–36410.

[35] S. Paik, S. Shak, G. Tang, C. Kim, J. Baker, M. Cronin, et al., A multigene assay to predict recurrence of tamoxifen-treated, node-negative breast cancer, N. Engl. J. Med. 351 (2004) 2817–2826.

[36] V.R. Jacobs, R.E. Kates, E. Kantelhardt, M. Vetter, R. Wuerstlein, T. Fischer, et al., Health economic impact of risk group selection according to ASCO-recommended biomarkers uPA/PAI-1 in node-negative primary breast cancer, Breast Cancer Res. Treat. 138 (2013) 839–850.

[37] M.P. Walker, M. Zhang, T.P. Le, P. Wu, M. Lainé, G.L. Greene, RAC3 is a pro-migratory co-activator of ERα, Oncogene. 30 (2011) 1984–1994.

[38] S.V. Yap, J.M. Koontz, A. Kontrogianni-Konstantopoulos, HAX-1: a family of apoptotic regulators in health and disease, J. Cell. Physiol. 226 (2011) 2752–2761.

[39] A. Mirmohammadsadegh, U. Tartler, G. Michel, A. Baer, M. Walz, R. Wolf, et al., HAX-1, identified by differential display reverse transcription polymerase chain

reaction, is overexpressed in lesional psoriasis, J. Invest. Dermatol. 120 (2003) 1045–1051.

[40] C. Sorino, V. Catena, T. Bruno, F. De Nicola, S. Scalera, G. Bossi, et al., Che-1/AATF binds to RNA polymerase I machinery and sustains ribosomal rRNA gene transcription, Nucleic Acids Res. 48 (2020) 5891–5906.

[41] M. Fanciulli, T. Bruno, M. Di Padova, R. De Angelis, S. Iezzi, C. Iacobini, et al., Identification of a novel partner of RNA polymerase II subunit 11, Che-1, which interacts with and affects the growth suppression function of Rb, FASEB J. 14 (2000) 904–912.

[42] A.N. Srinivas, D. Suresh, F. Mirshahi, P.K. Santhekadur, A.J. Sanyal, D.P. Kumar, Emerging roles of AATF: checkpoint signaling and beyond, J. Cell. Physiol. 236 (2021) 3383–3395.

[43] S. Iezzi, M. Fanciulli, Discovering Che-1/AATF: a new attractive target for cancer therapy, Front. Genet. 6 (2015) 141.

[44] T. Bruno, G. Corleone, V. Catena, C. Cortile, F. De Nicola, F. Fabretti, et al., AATF/Che-1 localizes to paraspeckles and suppresses R-loops accumulation and interferon activation in Multiple Myeloma, EMBO J 41 (2022), e109711.

[45] R.W.J. Kaiser, J. Erber, K. Höpker, F. Fabretti, R.U. Müller, AATF/Che-1-an RNA binding protein at the Nexus of DNA damage response and ribosome biogenesis, Front. Oncol. 10 (2020) 919.

[46] R.W.J. Kaiser, M. Ignarski, E.L. Van Nostrand, C.K. Frese, M. Jain, S. Cukoski, et al., A protein-RNA interaction atlas of the ribosome biogenesis factor AATF, Sci. Rep. 9 (2019) 11071.

[47] C. Barbato, N. Corbi, N. Canu, M. Fanciulli, A. Serafino, M. Ciotti, et al., Rb binding protein Che-1 interacts with Tau in cerebellar granule neurons. Modulation during neuronal apoptosis, Mol. Cell. Neurosci. 24 (2003) 1038–1050.

[48] C. Sorino, T. Bruno, A. Desantis, M.G. Di Certo, S. Iezzi, F. De Nicola, et al., Centrosomal Che-1 protein is involved in the regulation of mitosis and DNA damage response by mediating pericentrin (PCNT)-dependent Chk1 protein localization, J. Biol. Chem. 288 (2013) 23348–23357.

[49] T. Thomas, A.K. Voss, P. Petrou, P. Gruss, The murine gene, Traube, is essential for the growth of preimplantation embryos, Dev. Biol. 227 (2000) 324–342.

[50] C. Pisani, A. Onori, F. Gabanella, F. Delle Monache, A. Borreca, M. Ammassari-Teule, et al., eEF1Bγ binds the Che-1 and TP53 gene promoters and their transcripts, J. Exp. Clin. Cancer Res. 35 (2016) 146.

[51] M.G. Di Certo, N. Corbi, T. Bruno, S. Iezzi, F. De Nicola, A. Desantis, et al., NRAGE associates with the anti-apoptotic factor Che-1 and regulates its degradation to induce cell death, J. Cell Sci. England (2007) 1852–1858.

[52] J. Xie, Q. Guo, AATF protects neural cells against oxidative damage induced by amyloid beta-peptide, Neurobiol. Dis. United States (2004) 150–157.

[53] G. Page, I. Lödige, D. Kögel, K.H. Scheidtmann, AATF, a novel transcription factor that interacts with Dlk/ZIP kinase and interferes with apoptosis, FEBS Lett. 462 (1999) 187–191.

[54] J. Xie, Q. Guo, Apoptosis antagonizing transcription factor protects renal tubule cells against oxidative damage and apoptosis induced by ischemia-reperfusion, J. Am. Soc. Nephrol. 17 (2006) 3336–3346.

[55] A. Desantis, T. Bruno, V. Catena, F. De Nicola, F. Goeman, S. Iezzi, et al., Che-1-induced inhibition of mTOR pathway enables stress-induced autophagy, EMBO J. 34 (2015) 1214–1230.

[56] T. Bruno, A. Desantis, G. Bossi, S. Di Agostino, C. Sorino, F. De Nicola, et al., Che-1 promotes tumor cell survival by sustaining mutant p53 transcription and inhibiting DNA damage response activation, Cancer Cell 18 (2010) 122–134.

[57] A. Desantis, T. Bruno, V. Catena, F. De Nicola, F. Goeman, S. Iezzi, et al., Che-1 modulates the decision between cell cycle arrest and apoptosis by its binding to p53, Cell Death Dis. 6 (2015), e1764.

[58] V. Folgiero, C. Sorino, M. Pallocca, F. De Nicola, F. Goeman, V. Bertaina, et al., Che-1 is targeted by c-Myc to sustain proliferation in pre-B-cell acute lymphoblastic leukemia, EMBO Rep. 19 (2018).

[59] M. Sharma, Apoptosis-antagonizing transcription factor (AATF) gene silencing: role in induction of apoptosis and down-regulation of estrogen receptor in breast cancer cells, Biotechnol. Lett. 35 (2013) 1561–1570.

[60] N. Corbi, E.M. Batassa, C. Pisani, A. Onori, M.G. Di Certo, G. Strimpakos, et al., The eEF1γ subunit contacts RNA polymerase II and binds vimentin promoter region, PLoS One 5 (2010), e14481.

[61] F. Gabanella, A. Onori, M. Ralli, A. Greco, C. Passananti, M.G. Di Certo, SMN protein promotes membrane compartmentalization of ribosomal protein S6 transcript in human fibroblasts, Sci. Rep. 10 (2020) 19000.

[62] K. Lindfors, T. Halttunen, P. Huotari, N. Nupponen, M. Vihinen, T. Visakorpi, et al., Identification of novel transcription factor-like gene from human intestinal cells, Biochem. Biophys. Res. Commun. United States (2000) 660–666. Academic Press.; 2000.

[63] E.A. Grzybowska, V. Zayat, R. Konopinski, A. Trebinska, M. Szwarc, E. Sarnowska, et al., HAX-1 is a nucleocytoplasmic shuttling protein with a possible role in mRNA processing, FEBS J. 280 (2013) 256–272.

[64] J.A. Mobley, R.W. Brueggemeier, Estrogen receptor-mediated regulation of oxidative stress and DNA damage in breast cancer, Carcinogenesis. 25 (2004) 3–9.

[65] A. Nazmeen, S. Maiti, Redox Regulation of Estrogen Signaling in Human Breast Cancer, in: S. Chakraborti, B.K. Ray, S. Roychoudhury (Eds.), Handbook of Oxidative Stress in Cancer: Mechanistic Aspects, Springer, Singapore, 2022, https://doi.org/10.1007/978-981-15-9411-3_85.

[66] A. Trębińska-Stryjewska, M. Wakula, M. Chmielarczyk, E.A. Grzybowska, HAX1: a versatile, intrinsically disordered regulatory protein, Biochim. Biophys. Acta, Mol. Cell Res. 2023 (1870) 119538.

[67] D. Wang, T.Y. Chen, F.J. Liu, Che-1 attenuates hypoxia/reoxygenation-induced cardiomyocyte apoptosis by upregulation of Nrf2 signaling, Eur. Rev. Med. Pharmacol. Sci. Italy (2018) 1084–1093.

[68] S. Ishigaki, S.G. Fonseca, C.M. Oslowski, A. Jurczyk, J.R. Shearstone, L.J. Zhu, et al., AATF mediates an antiapoptotic effect of the unfolded protein response through transcriptional regulation of AKT1, Cell Death Differ. 17 (2010) 774–786.

[69] K. Yang, J. Yang, J. Yi, Nucleolar stress: hallmarks, sensing mechanism and diseases, Cell Stress 2 (2018) 125–140.

[70] R.T. Sapio, C.J. Burns, D.G. Pestov, Effects of hydrogen peroxide stress on the nucleolar redox environment and pre-rRNA maturation, Front. Mol. Biosci. 8 (2021) 678488.

[71] N. Shcherbik, D.G. Pestov, The impact of oxidative stress on ribosomes: from injury to regulation, Cells. 8 (2019).

[72] G. Nassa, G. Giurato, A. Salvati, V. Gigantino, G. Pecoraro, J. Lamberti, et al., The RNA-mediated estrogen receptor α interactome of hormone-dependent human breast cancer cell nuclei, Sci. Data 6 (2019) 173.

[73] P. Leister, S. Burgdorf, K.H. Scheidtmann, Apoptosis antagonizing transcription factor AATF is a novel coactivator of nuclear hormone receptors, Signal Transduct. 3 (2003) 17–25.

[74] Y. Xu, P. Huangyang, Y. Wang, L. Xue, E. Devericks, H.G. Nguyen, et al., ERα is an RNA-binding protein sustaining tumor cell survival and drug resistance, Cell 184 (2021), 5215-29.e17.

[75] W.J. Welboren, F.C. Sweep, P.N. Span, H.G. Stunnenberg, Genomic actions of estrogen receptor alpha: what are the targets and how are they regulated? Endocr. Relat. Cancer 16 (2009) 1073–1089.